Stable Photovoltaic Generation by Boost Converter via Adaptive ILQ Servo-Control

Yuichiro Nagano[#1], Sorawit Stapornchaisit[*2], Hiroshi Takami[#3], Sidshchadhaa Aumted[*4]

[#]*Electrical Engineering, Shibaura Institute of Technology*
3-7-5 Toyosu, Koto-ku, Tokyo 135-8548 Japan
[1]ma11119@shibaura-it.ac.jp
[3]takami@sic.shibaura-it.ac.jp

[*]*Thai-Nichi Institute of Technology*
1771/1, Pattanakarn Rd., Suanluang, Bangkok, 10250, Thailand
[2]sorawit.tni@gmail.com
[4]sidshchadhaa@tni.ac.th

***Abstract*— In this paper, we validate the adaptive voltage control strategy for boost converter via Inverse LQ Servo-Control is fitted for photovoltaic boost converter. Our presented strategy is based on an analytical formula of Inverse Linear Quadratic (ILQ) design method, which has characteristic of stability and robust control. We describe the resulting important properties of this design. Also we present the numerical simulations and the stability results in dynamical change of the input voltage.**

***Keywords*—boost converter, photovoltaic battery, optimal voltage control, inverse LQ design method, type-1 servo-system, adaptive control.**

I. INTRODUCTION

Nowadays, the range of the photovoltaic (PV) panel output voltage is between 24V and 48V for remaining underneath security voltage. These values are low when comparing with the necessary voltage at the inverter input. As a consequence the voltage gain of the DC/DC stage must be high enough to accommodate this difference[1]. Then, there are many studies proposed for boost converter as cascaded converters, transformer isolation, and quadratic boost converter [1]-[4].

The voltage-power characteristic of PV array is nonlinear and dynamic because of the changes caused by the atmospheric conditions. There are no studies about dynamic change of PV output to input boost converter.

The ILQ control system strategy is designed based on a linearized small-signal model and employed to control the power converters in which the ILQ design method is an optimal servo-system control without solving Riccati's equation [5]. Using this method, the transfer function can be asymptotically designed into specification. Hence, the optimal solution is guaranteed and the optimal gains can be adjusted at workplace [6]-[8]. The ILQ servo-control have characteristic as follow; very easy to designed, stable, robust and can be used as practical servo controller for the optimal electric control [9]-[12].

Recently, we proposed an adaptive voltage control strategy for boost converter via ILQ method with the stable photovoltaic generation. This strategy can control that validates stability operation of boost converter using the adaptive voltage control strategy for boost converter via ILQ method [13]. In this paper, the strategy is developed to stability operator in dynamic input voltage change. The paper is organized as follows. In this chapter describes the background of our study. Chapter II, the modeling, solving and finding of the ILQ Servo-System for the boost converter are presented. Chapter III, we present the numerical simulations and describe the resulting important properties of this design. Finally, the conclusion and the references are given.

II. MODEL AND PROPOSE CONTROL STRATEGY

In this step, we adopt the basic boost converter circuit as shown in Fig. 1 via the C-filter within the output circuit; the output voltage is equivalent to voltage source.

A. Modeling for the Boost Converter Circuit

The boost converter with PV battery is constituted of the power electronics components as shown in Fig. 1, and the equivalent circuit of boost converter is shown in Fig. 2, where v_1 is the input voltage, v_2 is the output voltage, i_1 is the input voltage, i_2 is the output current and i_c is the capacitor currents of the passive low-pass filter, respectively.

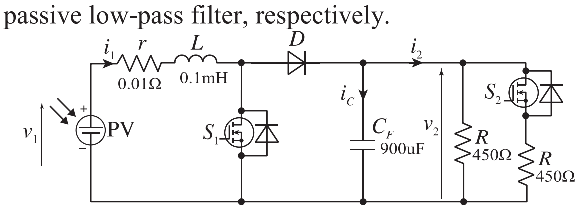

Fig. 1 The boost converter circuit

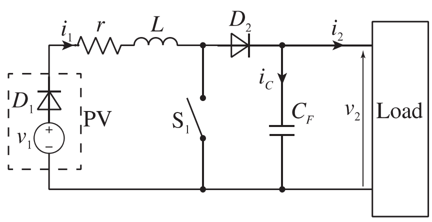

Fig. 2 Equivalent circuit of the boost converter

In this moment, the analytical boost converter is more difficult than the buck converter and the inverter, because the topology of boost converter is changed by switching based on the operation of inductor, MOSFET and diode D.

We can derive a linear state equation of the boost converter into two steps from Fig. 2 to find as follows; 1) deriving state equation, including time-variable duty-factor d_f into system matrix by state space average method, and 2) deriving time-invariant state equation by small signal analysis method.

B. Solving the Time-variant linear State Equation

The time-variant state average space model is consisted of average of a state space equation when the switch S_1 is "ON" period and a state space equation when the switch S_1 is "OFF" period.

Our synthesis of this boost converter based on the time intervals of length T_s, which is separated into "ON" period and "OFF" period by duty-factor d_f with the condition of $0 \le d_f \le 1$.

When the switch S_1 is the close circuit or called "ON" period, the current in the inductor L increases linearly and the switch S_2 is the open circuit in this period.

During the switch S_1 is the open circuit or called "OFF" period, the stored energy in the inductor L will be released through closed switch S_2 and the inductor creates the higher output voltage.

(i) The operation of switch can be represented by d_f to control the output voltage of v_2.

In the condition of $0\le t \le d_fT_s$ when the switch S_1 is "ON" period from Fig. 2, the circuit equations are given as follows:

$$v_1 = ri_1 + L\frac{di_1}{dt}, \quad v_2 = \frac{1}{C_F}\int i_c dt, \quad i_1 = i_2 + i_c. \tag{1}$$

In order to derive the state space equation, we reorganize the equation as follows:

$$\frac{di_1}{dt} = -\frac{r}{L}i_1 + \frac{1}{L}v_1 \tag{2}$$

$$\frac{dv_2}{dt} = -\frac{1}{C_F}i_2 \tag{3}$$

then we dispose the state space equation as follows:

$$\dot{x} = A_1x + B_1u + D_1d, \; y = C_1x \tag{4}$$

where

$x = \begin{bmatrix} i_1 & v_2 \end{bmatrix}^T$, $[\;\;]^T$ is transpose matrix, $u = v_1, d = i_2$,

$$A_1 = \begin{bmatrix} -\frac{r}{L} & 0 \\ 0 & 0 \end{bmatrix}, \; B_1 = \begin{bmatrix} \frac{1}{L} \\ 0 \end{bmatrix}, \; C_1 = \begin{bmatrix} 0 \\ 1 \end{bmatrix}^T, \; D_1 = \begin{bmatrix} 0 \\ -\frac{1}{C_F} \end{bmatrix}.$$

(ii) In the condition of   when the switch S_1 is "OFF" period from Fig. 2, the circuit equations are given as follows:

$$v_1 = ri_1 + L\frac{d}{dt}i_1 + v_2, \quad v_2 = \frac{1}{C_F}\int i_c dt, \quad i_1 = i_2 + i_c. \tag{5}$$

In order to derive the state space equation, we reorganize the equation as follows:

$$\frac{d}{dt}i_1 = -\frac{r}{L}i_1 - \frac{1}{L}v_2 + \frac{1}{L}v_1 \tag{6}$$

$$\frac{d}{dt}v_2 = \frac{1}{C_F}i_c = \frac{1}{C_F}i_1 - \frac{1}{C_F}i_2 \tag{7}$$

then we dispose the state space equation as follows:

$$\dot{x} = A_2x + B_2u + D_2d, \; y = C_2x \tag{8}$$

where

$$A_2 = \begin{bmatrix} -\frac{r}{L} & -\frac{1}{L} \\ \frac{1}{C_F} & 0 \end{bmatrix}, \; B_2 = \begin{bmatrix} \frac{1}{L} \\ 0 \end{bmatrix}, \; C_2 = \begin{bmatrix} 0 \\ 1 \end{bmatrix}^T \text{ and } D_2 = \begin{bmatrix} 0 \\ -\frac{1}{C_F} \end{bmatrix}$$

.

Finding the average state space equation indicated by duty-factor d_f and defining the new state variables as follows:

$$\left.\begin{aligned} A &= d_fA_1 + (1-d_f)A_2 \\ B &= d_fB_1 + (1-d_f)B_2 \\ C &= d_fC_1 + (1-d_f)C_2 \\ D &= d_fD_1 + (1-d_f)D_2 \end{aligned}\right\} \tag{9}$$

then considering the time-variant system, the average state equation can be rewritten from (9) as follows:

$$\dot{x} = Ax + Bu + Dd, \; y = Cx \tag{10}$$

where

$$A = \begin{bmatrix} -\frac{r}{L} & -\frac{1-d_f}{L} \\ \frac{1-d_f}{C_F} & 0 \end{bmatrix}, B = \begin{bmatrix} \frac{1}{L} \\ 0 \end{bmatrix}, C = \begin{bmatrix} 0 \\ 1 \end{bmatrix}^T \text{ and } D = \begin{bmatrix} 0 \\ -\frac{1}{C_F} \end{bmatrix}.$$

C. Finding the Time-invariant State Equation by small signal analysis method

According to the time-invariant system, a variable part of the duty-factor is important to separate by applying the superposition of the steady and the variable components for the state equation analysis as follows:

$$d_f = D_f + \Delta d_f \tag{11}$$

where D_f and Δd_f are the steady and the variable components of duty factor, respectively.

Substituting (11) to (10) yields:

$$A = \begin{bmatrix} -\frac{r}{L} & -\frac{1-(D_f+\Delta d_f)}{L} \\ \frac{1-(D_f+\Delta d_f)}{C_F} & 0 \end{bmatrix} = \Lambda + \Gamma\Delta d_f \tag{12}$$

where $\Lambda = \begin{bmatrix} -\frac{r}{L} & -\frac{1-D_f}{L} \\ \frac{1-D_f}{C_F} & 0 \end{bmatrix}, \; \Gamma = \begin{bmatrix} 0 & \frac{1}{L} \\ -\frac{1}{C_F} & 0 \end{bmatrix}.$

Thence, applying the steady state analysis with $\Delta d_f = 0$, the steady state equation can be obtained as follows:

$$\dot{x}_0 = \Lambda x_0 + Bu_0 + Dd_0 = 0 \tag{13}$$

where

$x_0 = \begin{bmatrix} I_1 & V_2 \end{bmatrix}^T$, $u_0 = V_1$, $d_0 = I_2$. I_1, I_2, V_1 and V_2 are average values of i_1, i_2, v_1 and v_2, respectively.

Then

$$-\frac{r}{L} I_1 - \frac{1-D_f}{L} V_2 + \frac{1}{L} V_1 = 0 \tag{14a}$$

$$I_1 = \frac{1}{1-D_f} I_2 . \tag{14b}$$

Substituting (14b) to (14a) and considering $0 \le D_f \le 1$ yield:

$$D_f = 1 - \frac{\frac{V_1}{V_2} + \sqrt{\left(\frac{V_1}{V_2}\right)^2 - 4r\frac{I_2}{V_2}}}{2} \approx 1 - \frac{V_1}{V_2} . \tag{15}$$

Because generally resistance r is very small, so we can neglect it. Taking account of $u = u_0 = V_1 = \text{constant}$ in (10), we consider about state variables as follows:

$$x = x_0 + \Delta x \tag{16a}$$

$$u = u_0 \tag{16b}$$

$$d = d_0 + \Delta d \tag{16c}$$

where Δx, Δd are variable components as:

$$\Delta x = x - x_0 = \begin{bmatrix} \Delta i_1 \\ \Delta v_2 \end{bmatrix} = \begin{bmatrix} i_1 - I_1 \\ v_2 - V_2 \end{bmatrix}, \ \Delta d = d - d_0 = \Delta i_2 = i_2 - I_2$$

Substituting (12) , (13) and (16a) - (16c) to (10) yields:

$$\begin{aligned} \Delta \dot{x} &= \left(\Lambda + \Gamma \Delta d_f\right)\left(x_0 + \Delta x\right) + Bu_0 + D\left(d_0 + \Delta d\right) \\ &= \Lambda \Delta x + \Gamma x_0 \Delta d_f + D\Delta d + \Gamma \Delta d_f \Delta x \end{aligned} \tag{17}$$

We can assume that $\Delta d_f \Delta x \approx 0$ on the small signal analysis, thus the time-invariant state equation is given as follows:

$$\dot{x}_s = A_s x_s + B_s u_s + D_s d_s , \ y_s = C_s x_s \tag{18}$$

where,

$x_s = \Delta x = \begin{bmatrix} \Delta i_1 & \Delta v_2 \end{bmatrix}^T$, $u_s = \Delta d_f$, $d_s = \Delta d = \Delta i_2$ and

$$A_s = \Lambda = \begin{bmatrix} -\frac{r}{L} & -\frac{1-D_f}{L} \\ \frac{1-D_f}{C_F} & 0 \end{bmatrix}, \ B_s = \Gamma x_0 = \begin{bmatrix} \frac{V_2}{L} \\ -\frac{I_1}{C_F} \end{bmatrix},$$

$$C_s = C = \begin{bmatrix} 0 & 1 \end{bmatrix} \text{ and } D_s = D = \begin{bmatrix} 0 & -\frac{1}{C_F} \end{bmatrix}^T$$

Henceforth, the plant must satisfy the controllable and observable system, the minimal-phase system, and the no zeros system at the origin, which already has all of conditions. We can verify and proof the system with the robust control theory approached [5], [6], [14].

D.Solving the Type-1 ILQ optimal Servo-System

In order to design the ILQ optimal servo-system, the following conditions is proposed [4], [8], [15], [16]:

- Proposed strategy extended the state feedback system.
- We can find the analytical optimal solution based on the ILQ design method.
- We can get the asymptotic feature of the ILQ optimal servo-system.
- We can follow the procedure for the optimal solutions of the ILQ servo-system.

In this section, we first derive the basic construction for the Type-1 ILQ servo-system, and then we explain about the procedure for getting the optimal gains of the Type-1 ILQ servo-system.

E. Finding the Basic Optimal Gains of the ILQ Servo-System

Fig. 3 shows a typical servo system, where y_s^* is a reference input, K_F is the feedback gain, K_I represents the integral gain of the servo controller.

Based on the conventional ILQ design method, the set of parameters of the basic ILQ servo-system represented in Fig. 4 are:

$$\begin{bmatrix} K_F & K_I \end{bmatrix} = V^{-1} \Sigma V \begin{bmatrix} K_F^0 & K_I^0 \end{bmatrix} \tag{19}$$

where K_F^0 and K_I^0 are the basic optimal gains, Σ is diagonal gain matrix as adjusting parameter, and V is suitable nonsingular matrix [7], [9], [17].

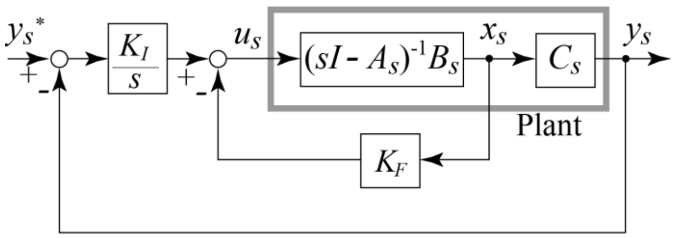

Fig. 3 Block diagram of typical servo-system

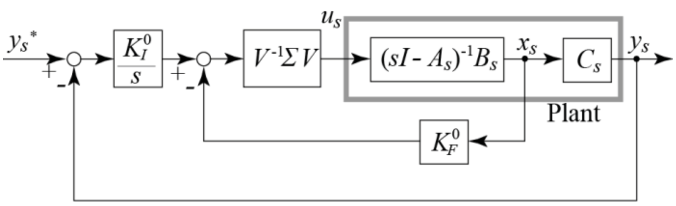

Fig. 4 Block diagram of construction of the ILQ servo-system

At this point we have achieved the optimal solutions of ILQ servo-system with gain K_F^0 and K_I^0.

F. Finding the Optimal Condition of the ILQ Servo-System and an adaptive control strategy

The ILQ servo-systems have the special property to converge the closed-loop transfer functions into objective decoupled- transfer functions. This idea leads to very simple adjustment of gains which is easier to control the servo-system.

Then, the basic gains K_F^0 and K_I^0 are derived by following procedures:

$$D_c := c_1 A^{d_1 - 1} B \tag{20}$$

where D_c, which must be nonsingular, i.e. necessary-and-sufficient condition, enables to decouple the system, c_1 is the 1st row-vector of matrix C, and $d_1 = \min\{k | c_1 A^{k-1} B \neq 0, k = 1,2,\ldots\}$ is the order difference between the denominator and the numerator of the plant.

The order difference, $d_1 = 2$ in the system was given by (20), so that the stable polynomial for $\phi_1(s)$ determines the response of the servo-system in the condition $\Sigma \rightarrow \infty$, can be defined as:

$$\phi_1(s) := \alpha_{1,1} + \alpha_{1,2} s + s^2 \tag{21}$$

where $\alpha_{1,1}$ and $\alpha_{1,2}$ are the coefficients of the polynomial, thus the objective transfer function is given by

$$G_1^{\infty}(s) = \frac{\phi_1(0)}{\phi_1(s)} = \frac{\alpha_{1,1}}{\alpha_{1,1} + \alpha_{1,2} s + s^2} \tag{22}$$

A polynomial matrix can be defined as:

$$N_\phi(A_s) = c_1 \phi_1(A_s) = c_1\left(\alpha_{1,1} + \alpha_{1,2} A_s + A_s^2\right)$$
$$= \begin{bmatrix} \frac{\alpha_{1,2}(1-D_f)}{C_F} - \frac{(1-D_f)r}{C_F L} & \alpha_{1,1} - \frac{(1-D_f)^2}{C_F L} \end{bmatrix} \tag{23}$$

then we can derive the decoupling gain as follows:

$$K = D_c^{-1} N_\phi(A_s) = \begin{bmatrix} \frac{r - \alpha_{1,2} L}{V_2} & \frac{\alpha_{1,1} C_F L - (1-D_f)^2}{(1-D_f) V_2} \end{bmatrix} \tag{24}$$

Consequently we can obtain the optimal basic gains as follows:

$$\begin{bmatrix} K_F^0 & \vdots & K_I^0 \end{bmatrix} = \begin{bmatrix} K & I \end{bmatrix} \begin{bmatrix} A_s & B_s \\ C_s & 0 \end{bmatrix}^{-1}$$
$$= \begin{bmatrix} \frac{L}{V_2} & \frac{\alpha_{1,2} L C_F}{(1-D_f) V_2} & \vdots & \frac{\alpha_{1,1} L C_F}{(1-D_f) V_2} \end{bmatrix} \tag{25}$$

In order to achieve a simple design of responses, we give objective transfer function of (22) as:

$$\alpha_{1,1} = \omega_n^2 \quad \text{and} \quad \alpha_{1,2} = 2\zeta\omega_n \tag{26}$$

where ω_n is natural angular velocity and ζ is damping coefficient.

The optimal condition can be calculated by following equation:

$$\Sigma > \frac{2(\alpha_{1,2} L - r)}{L} \tag{27}$$

From (25), basic gains K_F^0 and K_I^0, which are solved by analytical forms, are function of the steady component of duty factor D_f and voltage V_2, so that it enables to realize an adaptive control for varying the command output voltage y_s^*. Consequently we can derive a proposed adaptive ILQ servo-system as shown in Fig. 5. The adaptive arrow of the optimal basic gains K_F^0 and K_I^0 are indicated that they are adjusting themselves adaptively.

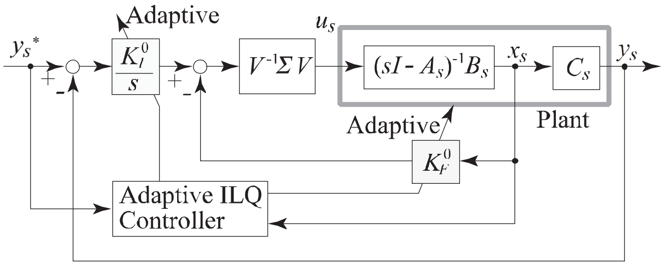

Fig. 5 Block diagram of construction of the adaptive ILQ servo-system for the stable photovoltaic generation by boost converter

III. Numerical Simulations and Results

Simulations were carried out at the condition of DC output voltage of 150V, the load resistance of 450Ω and the carried frequency of 100 kHz. The results of simulation are shown in Fig. 6 and Fig. 7. In case of Fig. 6, the input voltage changes between 10V and 16V in triangle waveform as the operating voltage range of photovoltaic battery. In Fig. 7, the input voltage waveform is similar to the output of photovoltaic battery. Both reference voltage is increased by 1V at 0.15s thenceforward, we changed back at 0.2s. Furthermore, the step-function load of 450Ω is connected to the output terminals at 0.25s for supplying the same disturbance load current. All of the simulation results were ω_n = 500, ζ = 0.707 and the optimal condition σ = 1000.

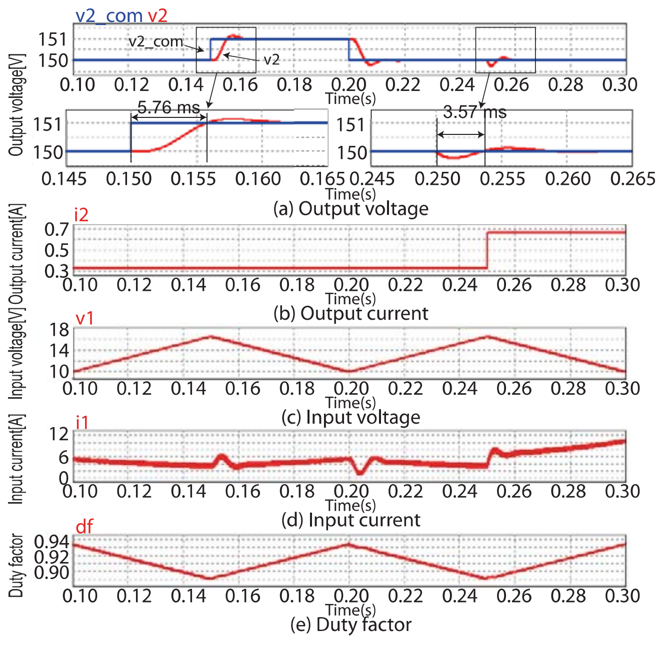

Fig. 6 The adaptive ILQ control with the stable photovoltaic generation (the input voltage v_1 changes triangle waveform)

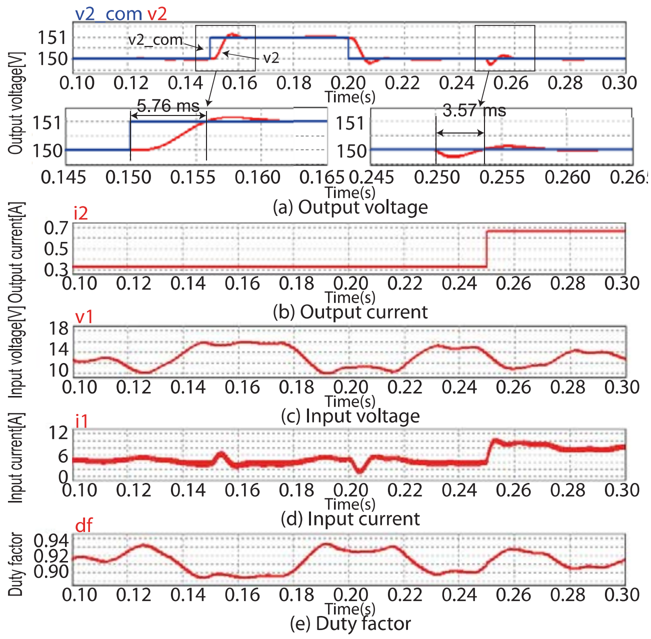

Fig. 7 The adaptive ILQ control with the stable photovoltaic generation (The input voltage v1 is similar to the output of photovoltaic battery)

The blue line represents the reference voltage and the actual voltage is represented by the red line, the output current, the input voltage, the output voltage, and the duty-factor of system is also presented.

For the evaluating response by the reference input, we define a "rising time", which is an interval from the increasing reference voltage output to 95% of the reference voltage. Moreover for the evaluating response by the disturbance of system, we define a "recovery time", which is an interval from the impact of its disturbance to the recovering level.

Considering Fig. 6 and Fig. 7, the rising times of the adaptive ILQ control with the photovoltaic generation with 2nd-order are 5.76ms, which means we can control the rising time with the properties of robust and insensitive of the disturbance of system. By comparing Fig. 6 and Fig. 7, we found that changing the amplitude of the input voltage from 10V to 16V, we can get the rising times are corresponded to 5.76ms, due to adaptive control of D_f and the reference voltage v_2*, which determines the voltage transformation ratio. This means that the optimal gains of our proposed controller are changed automatically and adaptively.

Considering all results, the duty-factor in (c) are fallen in the controlling region in range of (0,1) are stable and under control.

IV. Conclusion

We have proposed the stable control strategy for the photovoltaic boost converter by using the adaptive ILQ servo control with the optimal gains of system, which the time response and the disturbance response are dynamically controlled by a single parameter, ω_n .

In general, the boost converter voltage step-up ratio is up to 10 times. Our control strategy can stability operates the voltage step-up ratio up to 37.5 times in a basic converter. But in this condition duty factor is almost theoretical value 0.98, the input current is definitely high, so that it leads to low efficiency.

Next step, this problem will be solved by using practical quadratic boost converter circuit [1], [4].

References

[1] Riad KADRI, Jean-Paul GAUBERT, Gerard CHAMPENOIS, Mohamed MOSTEFAI, "Performance Analysis of Transformless Single Switch Quadratic Boost Converter for Grid Connected Photovoltaic Systems," *XIX International Conference on Electrical Machines*, *ICEM 2010*, Rome.

[2] Geoffrey R. Walker, Paul C.Sernia, "Cascaded DC-DC Converter Connection of Photovoltaic Modules," *IEEE Transactions on Power Electronics*, Vol.19, No.4, July 2004.

[3] Yang Haizhu, Liu Jie, "Research on Maximum Power Point Tracking Control Based on the Low Power Photovoltaic Grid-connected Inverter," *IPEMC 2009*, 978-1-2422-3557-9/09

[4] Ping Yang, Jianping Xu, Guohua Zhou, Shiyu Zhang, "A New Quadratic Boost Converter with High Voltage Step-up Ratio and Reduced Voltage Stress," 2012 IEEE 7th International Power Electronics and Motion Control Conference – ECCE Asia, June 2-5, 2012, Harbin, China

[5] T. Fujii, "A New Approch to the LQ Design from the Viewpoint of the Inverse Regulator Problem," *IEEE Trans. Automatic Control,* vol. AC-32, no. 11, Nov 1987, pp. 995-1004.

[6] T. Fujii, Y. Nishimura, S. Shimomura, and S.Kawarabayashi, "A Practical Approach to LQ Design and Its Application to Engine Control," *Proc. IFAC'87, Munich,* 1987, pp. 253-258.

[7] H. Kimura, T. Fujii, and T. Mori, Robust Control. Tokyo: Corona Publishing Co., Ltd, pp. 109-156, 1994.

[8] H. Takami, "Robust Current Control for Permanent Magnet Synchrous Motors by the Inverse LQ Method -An Evaluation of Control Performance Using Servo-Locks at Low Speed-," *Journal of power Electronics,* vol. 4, no.4, Oct. 2004, pp. 228-236.

[9] S. Aumted, S. Kanda, H. Takami, and S. Tatsuno, "Optimal Voltage Control for Single-Phase Inverter with Resonant LC Filter by Type-2 ILQ Servo-Control by 2nd-Order Polynomial," *Applied Mechanics and Materials Journal: Trans Tech Publications, Switzerland,* 2013, vol. 622-623, pp. 1514-1518 [*ICMCE 2012 Conf. Shanghai,* Aug. 2012].

[10] H. Takami, "Optimal Unity Power Factor control of Permanent Magnet Synchronous Motor with q-axis Field by Inverse LQ Method," *ISSN Journal of power Electronics.* Vol. 1, No.2, Oct, 2001, pp. 117-126.

[11] H Takami, "Design of an optimal servo-controller for current control in a permanent magnet synchronous motor," *Proc. IEE -Control Theory appl.,* vol 149, No. 6 Nov. 2002, pp. 564-572.

[12] H. Takami and M. Nakagawa, "Optimal Robust Current Control of Three Phase Induction Motor by ILQ Design Method," *Proc. ICEMS 2006 DS2E-07,* 2006.

[13] S. Stapornchaisit, S. Aumted, H. takami "A Novel Adaptive Voltage Control Strategy for Boost Converter via Inverse LQ Servo-Control," in *WASET '12 Phuket, Thailand International Conference Program*, Dec 25-27, 2012, Phuket, Thailand.

[14] T. Fujii, S. Kunimatsu, and O. kaneko, "Synthesis of ILQ Control System for Disturbance Attenuation," in *Proc. SICE Annual Conference*, Japan, 2008, pp. 1300-1303.

[15] T. Fujii, and T. Shimomura, "Generalization of ILQ Method for the Design of Optimal Servo Systems," *Trans. of the Institute of Systems, Control and Information Eng.* vol. 1, no. 6, pp.194-203, 1988.

[16] T. Shimomura, T. Fujii, and N. suda, "Generalization of the ILQ Regulator Design Method," in *Proc. American Control Conference,* Seattle, 1995, pp. 1967-1968.

[17] T. Fujii, "Design of Tracking Systems with LQ Optimality and Quadratic Stability," in *Proc. IFAC World Congress, IFAC'93*, Sydney, 1993, pp. 435-442.